The Plant Cell, Vol. 11, 2331–2347, December 1999, www.plantcell.org © 1999 American Society of Plant Physiologists

Organized F-Actin Is Essential for Normal Trichome Morphogenesis in Arabidopsis

Daniel B. Szymanski,[a,1] M. David Marks,[b,c,d] and Susan M. Wick[c]

[a] Department of Agronomy, Purdue University, 1150 Lilly Hall of Life Sciences, West Lafayette, Indiana 47907-1150
[b] Department of Genetics and Cell Biology, University of Minnesota, 1445 Gortner Avenue, St. Paul, Minnesota 55108-1095
[c] Department of Plant Biology, University of Minnesota, St. Paul, Minnesota 55108
[d] Plant Molecular Genetics Institute, University of Minnesota, St. Paul, Minnesota 55108

Actin microfilaments form a three-dimensional cytoskeletal network throughout the cell and constitute an essential throughway for organelle and vesicle transport. Development of Arabidopsis trichomes, unicellular structures derived from the epidermis, is being used as a genetic system in which to study actin-dependent growth in plant cells. The present study indicates that filamentous actin (F-actin) plays an important role during Arabidopsis trichome morphogenesis. For example, immunolocalization of actin filaments during trichome morphogenesis identified rearrangements of the cytoskeletal structure during the development of the mature cell. Moreover, pharmacological experiments indicate that there are distinct requirements for actin- and microtubule-dependent function during trichome morphogenesis. The F-actin–disrupting drug cytochalasin D does not affect the establishment of polarity during trichome development; however, maintenance and coordination of the normal pattern of cell growth are very sensitive to this drug. In contrast, oryzalin, an agent that depolymerizes microtubules, severely inhibits cell polarization. Furthermore, cytochalasin D treatment phenocopies a known class of mutations that cause distorted trichome morphology. Results of an analysis of cell shape and microfilament structure in wild-type, mutant, and drug-treated trichomes are consistent with a role for actin in the maintenance and coordination of an established growth pattern.

INTRODUCTION

Differentiation and growth of plant cells are under complex regulation. Information from multiple inputs controls the identity and form of each cell. For example, in both the root and shoot epidermis, hormone amounts, extrinsic positional cues, and developmental programs combine to regulate cell fate and morphogenesis of trichoblasts (Dolan et al., 1993; Larkin et al., 1994, 1996, 1997; Masucci et al., 1996; Szymanski et al., 1998). The mechanism by which positional information and cell fate decisions lead to changes in cell structure is not known. However, many examples in the literature demonstrate the importance of both actin and actin binding proteins in the control of cell shape (reviewed in Heslop-Harrison et al., 1986; McCurdy and Williamson, 1991; Staiger et al., 1997). Clearly, a complex signal transduction pathway must regulate the structure and dynamics of the cytoskeleton in response to these and other signals. Significant progress has been made in understanding how plant cells perceive signals (Baker et al., 1997; Fankhauser and Chory, 1997; Woeste and Kieber, 1998), but little is known about how signal perception leads to an appropriate morphogenetic response. The results of this study establish the utility of Arabidopsis trichome development as a model process in which to identify and study the genes involved in filamentous actin (F-actin)–dependent cell growth.

Arabidopsis trichomes are unicellular structures that arise from epidermal precursors. The genetic control of trichome development has been well characterized (Hülskamp et al., 1994; Folkers et al., 1997; reviewed in Marks, 1997). The pathway can be conceptually divided into three functional units: initiation promotion, initiation inhibition, and morphogenesis control. Furthermore, the trichome development pathway is intimately linked to leaf developmental status, and a relationship between the control of trichome initiation and cell cycle status has been found in several studies (Pyke et al., 1991; Lloyd et al., 1994; Szymanski and Marks, 1998). The *GLABROUS1* (*GL1*) and *TRANSPARENT TESTA GLABRA* (*TTG*) genes regulate entry into the trichome pathway, playing a role (reviewed in Marks, 1997) in both the initiation and inhibition pathways. With respect to trichome morphogenesis, the homeodomain-containing gene *GL2* and the *GL3* gene appear to act downstream of *GL1* and *TTG* but are epistatic to most of the genes that regulate trichome morphogenesis. *GL2* and *GL3* may function as master regulatory

[1] To whom correspondence should be addressed. E-mail dszyman@purdue.edu; fax 765-496-2926.

genes that control a complex morphogenic pathway. Therefore, the Arabidopsis trichome presents a good system in which to use genetic and molecular tools to examine the relationship between differentiation signals, the cytoskeleton, and the control of cell growth. For example, mutation in the *ZWICHEL* (*ZWI*) gene leads to defects in cell expansion and branching during trichome morphogenesis (Oppenheimer et al., 1997). Biochemical experiments have shown that *ZWI* encodes a calmodulin-regulated kinesin-like motor protein (Song et al., 1997; Narasimhulu and Reddy, 1998). The presence of at least 23 additional loci affecting trichome morphology suggests that several candidate cytoskeleton regulatory genes have yet to be identified (reviewed in Marks, 1997).

Analogous genetic studies of bristle morphology mutants in Drosophila have provided a way to examine the in vivo function of F-actin–regulatory proteins in a multicellular organism. In contrast to Arabidopsis trichomes, the mature Drosophila bristle is an unbranched hollow cell that dies upon maturity. The macrochaeta functions as a motion detector in a multicellular sensory complex. The specialized requirements for F-actin assembly during bristle development have been exploited to identify several genes that regulate microfilament organization. For example, severe *singed* alleles cause female sterility and hair defects (Bender, 1960). The predicted protein product of the *SINGED* gene shares amino acid similarity with the actin-bundling protein FASCIN and may play a direct role in actin bundle assembly during bristle formation (Cant et al., 1994; Tilney et al., 1995). Removal of the profilin- or actin-capping protein genes is lethal in Drosophila. However, weak mutant alleles of both of the genes yield bristle defects (Verheyen and Cooley, 1994; Hopmann et al., 1996).

Genetic approaches to analyze F-actin–dependent processes in plant cells have enormous potential (Gilliland et al., 1998). The importance of actin in polar responses in plant and algal cells has been established for many cell types. An intact microfilament system is essential for vesicle transport and cell growth. Actin also plays an important role during differentiation and morphogenesis. For example, the orientation of cell divisions during stomatal development is affected by cytochalasins (Cho and Wick, 1990, 1991; Palevitz, 1993). Also, proper actin organization is essential for normal establishment of polarity in the embryos of the brown algae Fucus and Pelvetia; pharmacological experiments with cytochalasins indicate that an unperturbed F-actin cytoskeleton is required for the normal onset of cell polarization in Fucus embryos (Quatrano, 1973; Brawley and Robinson, 1985). In Pelvetia, an F-actin patch in living embryos has been reported as an early marker of cell polarization, predicting the position of rhizoid emergence (Alessa and Kropf, 1999). In contrast to the dramatic effect of cytochalasins, the microtubule-destabilizing drug oryzalin has a very modest effect on cell polarization in Pelvetia (Hable and Kropf, 1998; Alessa and Kropf, 1999). Pharmacological evidence and F-actin localization also suggest that actin plays an important role during pollen germination (Mascarenhas and LaFountain, 1972; reviewed in Heslop-Harrison et al., 1986). In the germinated pollen tube, a complex longitudinal array of microfilaments is present and essential for the maintenance of polar growth (Picton and Steer, 1981; Lancelle et al., 1987; Miller et al., 1996; Kost et al., 1998).

In this study, we demonstrate the importance of F-actin during Arabidopsis trichome morphogenesis. Immunolocalization of actin in developing trichomes detected several organized F-actin arrays. The organization of these arrays depended on both the developmental stage of the trichome and the location within the cell. Moreover, trichome morphogenesis appears to have stage-specific functional requirements for the microtubule and actin cytoskeletons. The microtubule-destabilizing drug oryzalin inhibits the onset of cell polarization, and cytochalasin D inhibits the maintenance of cell shape later in trichome morphogenesis. Interestingly, cytochalasin D treatment phenocopies the trichome shape defects seen in the "distorted" class of mutants. F-actin organization in the distorted mutant *gnarled* (*grl*) displays clear differences compared with that of the wild type both early and late in trichome development.

RESULTS

Trichome Measurements

Trichome development has been divided into six discrete stages based on specific morphological landmarks (Szymanski et al., 1998). However, the cell shape changes that occur during morphological transitions have not been characterized in detail. This information is important because it reveals localized changes in cell expansion that occur within and between specific stages of growth. Therefore, stalk and branch dimensions of developing wild-type trichomes were measured to examine possible cell size constraints during trichome growth and to characterize the nature and extent of cell expansion in each phase (Figure 1). Comparison of cell-shape defects in mutant and drug-treated cells is an important part of this study. Therefore, measurements of wild-type trichomes also served as a standard to characterize the specific shape defects of mutant and drug-treated trichomes.

Scanning electron microscopic images of a population of trichomes at different developmental stages were collected, and the length and diameter of trichome stalks and branches were measured. For spherical trichome precursors and polarized cells that had not initiated branches, cell length or stalk length was defined as the total visible height of the cell. Static images of developing trichomes do not make clear to what extent the cell wall material near the tip of the cell at the branch junctions is stalk or branch derived. Therefore, for branch-containing cells, the trichome stalk

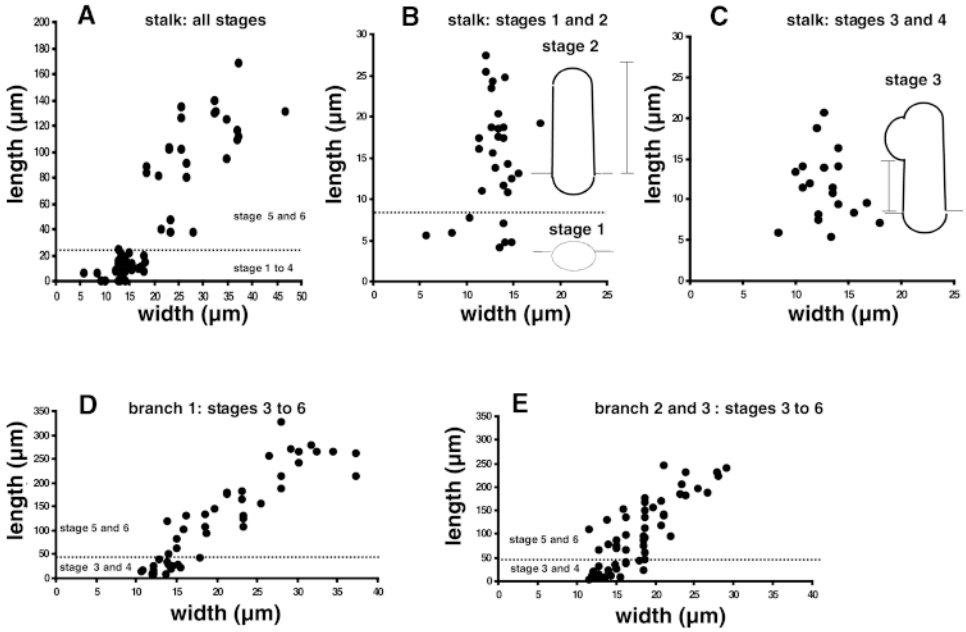

Figure 1. Dimensions of Trichome Cell Length and Width at All Major Developmental Stages.

Measurements were taken from static images of a population of trichomes. Each plot graphs the length of the trichome branch or stalk in the y axis and the width in the x axis. Stalk length is defined as the distance from the base of the cell to the tip; for trichomes with branches, the stalk is defined as the distance from the plane of the epidermis to the lowest surface of the first branch.

(A) Trichome stalks at all stages of development. The dashed line defines the division in cell size between trichomes up to stage 4 and stage 5 cells.

(B) Trichome stalk measurements in stage 1 and stage 2 trichomes and sketches of stage 1 and stage 2 trichomes. The vertical line adjacent to the sketch of the stage 2 cell demonstrates the measurement of stalk length. The dashed line defines the division in cell size between stage 1 and stage 2 cells.

(C) Trichome stalk measurements in stage 3 trichomes and sketch of a stage 3 trichome. The vertical line adjacent to the sketch demonstrates the measurement of stalk length in a stage 3 trichome.

(D) Measurements of trichome branch 1 width at the branch base and length at all stages of development. The dashed line indicates the division between developmental stages as indicated.

(E) Measurements of trichome branch 2 and branch 3 width at the branch base and length at all stages of development. The dashed lines indicate the division between developmental stages as indicated.

was defined as the portion of the cell from the upper surface of the epidermis to the lowest surface of the lowest branch, providing a minimum estimate of stalk length. The plot of stalk length relative to width for all stages of trichome development shows a general positive correlation but has a considerable degree of scatter (Figure 1A). Closer examination of the early stages of trichome morphogenesis indicated that the positive correlation between increases in cell length and width did not hold for all stages of development and that cell geometry was highly constrained during early developmental stages. For example, stage 1 trichomes, defined as radially expanded cells within the epidermis, were found in fields of cells that had typical angular cell walls. Stage 1 persists until cells are $\sim$12 μm wide and reach $\sim$8 to 10 μm above the upper surface of the epidermis (Figure 1B). Stage 2 covers the transition to polar expansion perpendicular to the plane of the leaf. Trichome diameter did not increase greatly during stage 2, but stalk length increased from $\sim$10 to 28 μm. No stage 2 trichomes $>$30 μm were detected.

During stage 3 of trichome development, branch initiation occurs. Branch initiation occurs sequentially on the trichome stalk so that a single cell often has branches at slightly different developmental stages. For example, stage 4 trichomes, defined as cells that have expanded branches with a blunt tip, often contain both initiating branch buds and elongated branches with blunt tips. In most cases, three branch initiation events were observed on the developing stalk. Stalk length and diameter in a population of stage 3 and 4 trichomes are graphed in Figure 1C. During stage 3,

initiating branches appear on the lateral face of the stalk as diffuse circular regions of cell expansion with an initial diameter of ~10 μm (Figures 1D and 1E). Because the stalk is defined as the region between the branch and the epidermal surface, the plot of cell dimensions for stage 3 and 4 trichomes showed that their length was less than that in stage 2 (Figure 1C). None of the stage 3 cells observed had a stalk length equal to 25 μm, a length often reached in stage 2 trichomes (Figure 1B). This difference in length reflects the lateral position of a branch bud that eventually consumes a portion of the length of the stalk and indicates that the initiating branch does not arise from a point on the tip of a stage 2 trichome.

The order of branching in stage 4 cells can be determined on the basis of differences in size. In many cases, the first branch, defined as the primary branch, emerges from the trichome stalk and often points toward the proximal end of the leaf (Hülskamp et al., 1994). The second and third branches, defined as secondary, often point toward the distal end of the leaf. To examine possible differences in the growth characteristics of branch 1 and branches 2 and 3, we measured the dimensions of each independently.

Each of the developing branch buds appeared as circular regions of cell expansion ~10 μm in diameter on the trichome surface (Figures 1D and 1E). Through stage 4, branch expansion was limited in scope; the transition out of stage 4 occurred well before the developing trichome reached its final size (Figures 1A, 1D, and 1E). Stage 5 trichomes are defined as cells that contain branches with fine tips, and branch and stalk expansion during stage 5 yielded the vast majority of the volume of the cell. The extent of growth during stage 5 was variable from cell to cell. At stage 6, cell expansion is completed, and the cell wall acquires a papillate surface. Stalk length in mature stage 6 cells varied from 48 to 160 μm. The dimensions of the first branch to form did not substantially differ from those of the later branches. Branch 1 lengths varied from 118 to 325 μm, and branch 2 and branch 3 lengths varied from 112 to 248 μm.

Immunolocalization of Actin in Developing Trichomes

To begin to characterize the involvement of the actin cytoskeleton in trichome development, we immunolocalized actin in whole-mounted, permeabilized trichomes. These immunolocalization methods represent a slightly modified version of the freeze-shattering protocol described by Wasteneys et al. (1997).

Immunolocalizations of the most prominent actin-containing structures in trichomes from stages 1 to 6 are shown in Figure 2. Several members of the actin gene family are expressed in trichomes (An et al., 1996a, 1996b; McDowell et al., 1996); because the contribution of each gene product to the actin signal is not known, our results are interpreted as a summed actin signal. In Figures 2A to 2I, each image is a maximum projection of confocal optical sections that include the cell or cells of interest. The signal in Figures 2A to 2H can be compared with that in Figure 2I, which displays background fluorescence in the absence of the primary antibody. F-actin was detected in both stage 1 trichomes and adjacent socket cells. In the stage 1 trichome, a reticulating lattice of F-actin that linked the cell center and the cortex was detected (Figure 2A). A subset of the signal shown in Figure 2A was derived from cortical actin filament arrays. This pattern of actin organization is clearly demonstrated in the spherical stage 1 trichome shown in Figure 2B.

The arrangement of F-actin in stage 2 trichomes displayed stratification along the long axis of the cell (Figure 2C). Diffuse actin and several loosely aligned F-actin strands were detected in the developing stalk and were not limited to the cortex. In the tip region of the stalk, F-actin was less prominent, with most of the actin signal arising from small spherical bodies of unknown identity.

During stages 3 and 4, most of the actin signal came from the region of the cell in which branches were initiating or developing. Actin immunofluorescence in three branches of slightly different developmental stages is shown in the stage 4 trichome in Figure 2D. Much of the extremely strong actin signal detected in the initiating branch bud 3 (Figure 2D) was associated with spherical bodies. Because of the intensity and complexity of the signal associated with initiating branches, detection of ordered F-actin structures in this region of the cell was difficult, and attempts to visualize F-actin in living trichomes by using labeled phalloidins were not successful. In the next older branch (Figure 2D, br2), which had stage 4 morphology, diffuse actin labeling was detected in a broad (~8 μm diameter) region of cytoplasm that extended toward the tip. Numerous fine F-actin strands were loosely aligned with the future long axis of the developing branch. Similar fine F-actin strands and a diffuse actin signal were detected in the oldest branch within the same cell (Figure 2D, br1). However, there were fewer actin bundles near the branch tip than there were in earlier stages.

F-actin localization was most problematic during stage 5 of trichome morphogenesis. In most cases, aldehyde fixation of stage 5 trichomes yielded a strong but diffuse actin signal that was detected throughout the cytoplasm and in association with putative vacuolar compartments. Fixation in methanol was more effective in preserving F-actin during this stage of trichome morphogenesis. A dense meshwork of extremely fine F-actin strands was detected in the stalk and branches in stage 5 trichomes (Figure 2E). The alignment of F-actin during stage 5 was difficult to determine, but higher magnification of branches resolved actin filaments or bundles along the length of the developing branches (data not shown).

Mature stage 6 trichomes can be recognized in confocal images by the long wavelength autofluorescence of the papillate trichome cell wall. F-actin localization in mature trichomes revealed an intricate three-dimensional cytoskeletal network with actin bundles in the stalk and branches in a net parallel orientation relative to the long axis of each (Figure

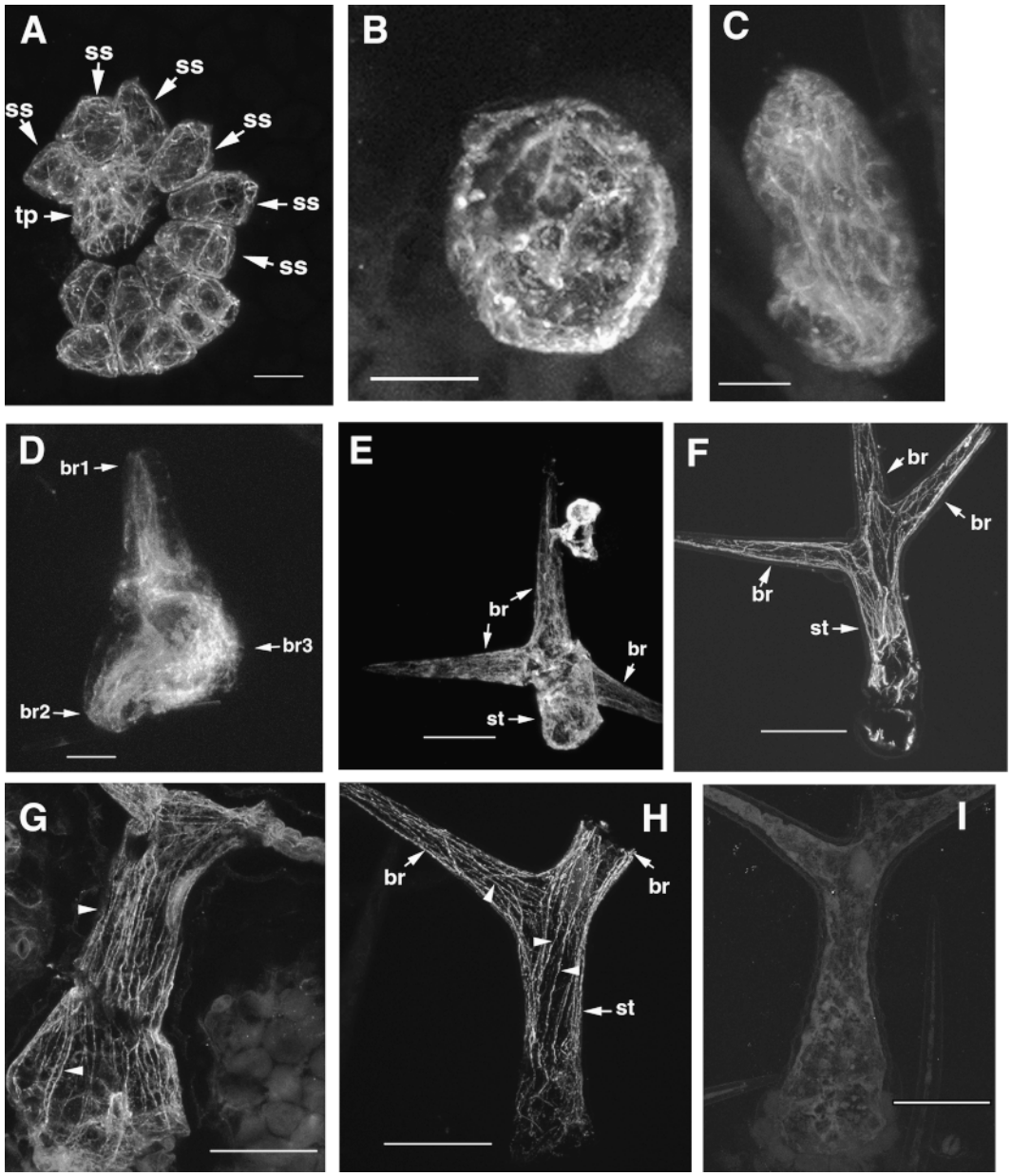

Figure 2. Actin Immunolocalization in Trichomes at Stages 1 to 6.

(A) to **(I)** each contain a maximum projection of a stack of confocal images.
(A) Top view of a stage 1 trichome precursor and surrounding socket cells.
(B) Top view of an isodiametric stage 1 trichome.
(C) Side view of a late stage 2 trichome.
(D) Top view of a trichome at stage 3, during the transition from branch initiation to branch growth. Branches are numbered on the basis of differences in size.
(E) Side view of a detached stage 5 trichome including a portion of the stalk and two intact branches.
(F) Side view of an intact stalk and the junction that contains the base of three branches.
(G) Side view of a stage 6 trichome stalk.
(H) Side view of stage 6 trichome stalk and branch.
(I) Control immunolocalization performed without primary antibody.
Arrowheads indicate cortical actin filaments. br, branch; ss, socket cell; st, stalk; tp, trichome precursor. Bars in **(A)** to **(D)** = 10 μm; bars in **(E)** to **(I)** = 50 μm.

2F). Higher magnification of the stalk of a stage 6 trichome detected numerous fine F-actin bundles that aligned with the long axis of the stalk and were somewhat evenly spaced along the circumference (Figure 2G). Many actin filaments or filament bundles >100 μm long extend in an ordered manner from the stalk into the overlying branch (Figure 2H). In the mature trichome, most of the inner cell volume is occupied by vacuole. Medial longitudinal optical sections indicated that almost all the signal shown in Figures 2F, 2G, and 2H is cortical (data not shown).

Organized F-Actin Is Important for Trichome Morphogenesis

It is not known whether any of the actin observed throughout trichome development is involved in the control of cell shape. To test for a role of F-actin during trichome growth, we treated developing Arabidopsis leaves with cytochalasin D.

Cytochalasin D binds either to the ends of actin filaments or to the actin monomer and disrupts F-actin organization in vivo (reviewed in Cooper, 1987). Control leaves treated for 48 hr with buffer containing 0.1% DMSO had trichomes with normal branch positions and stalk and branch geometry (Figure 3A). An example of a wild-type stage 4 trichome is labeled in Figure 3B. When leaves at a similar developmental stage were treated for 48 hr with 50 μm cytochalasin D, defects in trichome morphology were apparent (Figure 3C). In the presence of cytochalasin D, many trichome stalks and branches on the adaxial surface were twisted and asymmetrical. However, stage 6 cells were not noticeably affected. Presumably, the shape of the fully developed trichomes was already established at the time of cytochalasin D treatment, and cell morphology was no longer affected by the drug, even though F-actin arrays were affected in these cells (Figure 3F).

High magnification of a developing stage 4 trichome shown in Figure 3C revealed severely altered stalk expansion after cytochalasin D treatment relative to untreated controls (Figure 3D). The stalk was swollen, with a diameter of ~30 μm, approximately twice that of a representative normal trichome at a similar developmental stage.

Extended cytochalasin D incubation times disrupted cell morphology but did not completely inhibit growth (Figure 3E). In some cases, cell length and stalk diameter were comparable with those of controls, but most often, long-term cytochalasin D–treated cells were bulged or twisted. The coordination of stalk and branch growth and branch position was markedly altered by cytochalasin D treatment. Often, abortive branches were observed near the stalk base and at the apex of the trichome (Figure 3E). Figure 3E shows elongated branches at the cell apex. Similar effects on trichome morphogenesis were observed in leaves treated with another microfilament-destabilizing drug, latrunculin B (data not shown).

To confirm the effect of cytochalasin D treatment on actin microfilaments, we conducted immunolocalization studies. Abnormalities in F-actin organization were commonly seen in cytochalasin D–treated cells at all stages of development (data not shown); the trichome shown in Figure 3F is in stage 6. Strongly fluorescent actin rods of variable length were detected in the stalk and branches. In addition, a punctate actin signal was often observed at the cell cortex. The time course of cytochalasin D penetration and F-actin disruption was also determined. Three replicate experiments indicated that after 30 min of cytochalasin D treatment, F-actin in the stalk of stage 6 cells was completely fragmented and disorganized (data not shown). Between 2 and 24 hr of drug treatment, F-actin appeared to aggregate into heavy bars, as shown in Figure 3F.

Cytochalasin D treatment clearly has an effect on morphogenesis at several stages of development. However, using leaves from wild-type plants, we were not able to determine the developmental stage of individual trichomes at the time of drug treatment. This technical barrier hindered our ability to address whether there is a requirement for an unperturbed actin cytoskeleton during the onset of polarity. Therefore, we used a transgenic line in which trichome initiation was under the control of a dexamethasone-inducible form of the maize *R* gene (*ttg* 35S::*R-GR*) to examine the role of F-actin and microtubules at the onset of polarization during trichome initiation (Lloyd et al., 1994). Control plants treated with 0.1% DMSO alone did not initiate trichomes (Figure 4A). Additional control experiments showed that none of the cytoskeleton-disrupting agents, either alone or in combination, bypassed dexamethasone-dependent initiation (data not shown). Treatment of *ttg* 35S::*R-GR* plants with dexamethasone caused widespread trichome initiation on the adaxial epidermis (Figure 4B). Induced trichomes displayed polarized growth in both developing stalks and branches. However, many of the induced trichomes had smaller stalks and fewer branches than the wild type. Despite these morphological differences, the stalks and branches of induced trichomes contained longitudinal actin bundles that ran in an organized manner from the cell base into the branches (Figure 4C). The most noticeable difference between F-actin organization in induced trichomes and the trichomes that arise during normal development was the number of parallel filaments in the stalk.

To test the requirement for an unperturbed actin cytoskeleton during trichome initiation and branch formation, we performed dexamethasone induction on leaves that were either pretreated or simultaneously treated with cytoskeletal inhibitors. In induction experiments, pretreatment and simultaneous treatment with cytoskeletal inhibitors gave the same results. Cytochalasin D treatment did not appear to inhibit trichome initiation, because the numbers of induced trichomes in cytochalasin D–treated leaves were similar to those in the controls (Figure 4D). Furthermore, the developing trichomes displayed polar outgrowth and branch initiation; trichomes with two or three branches were detected in cytochalasin D–treated cells. However, some trichomes

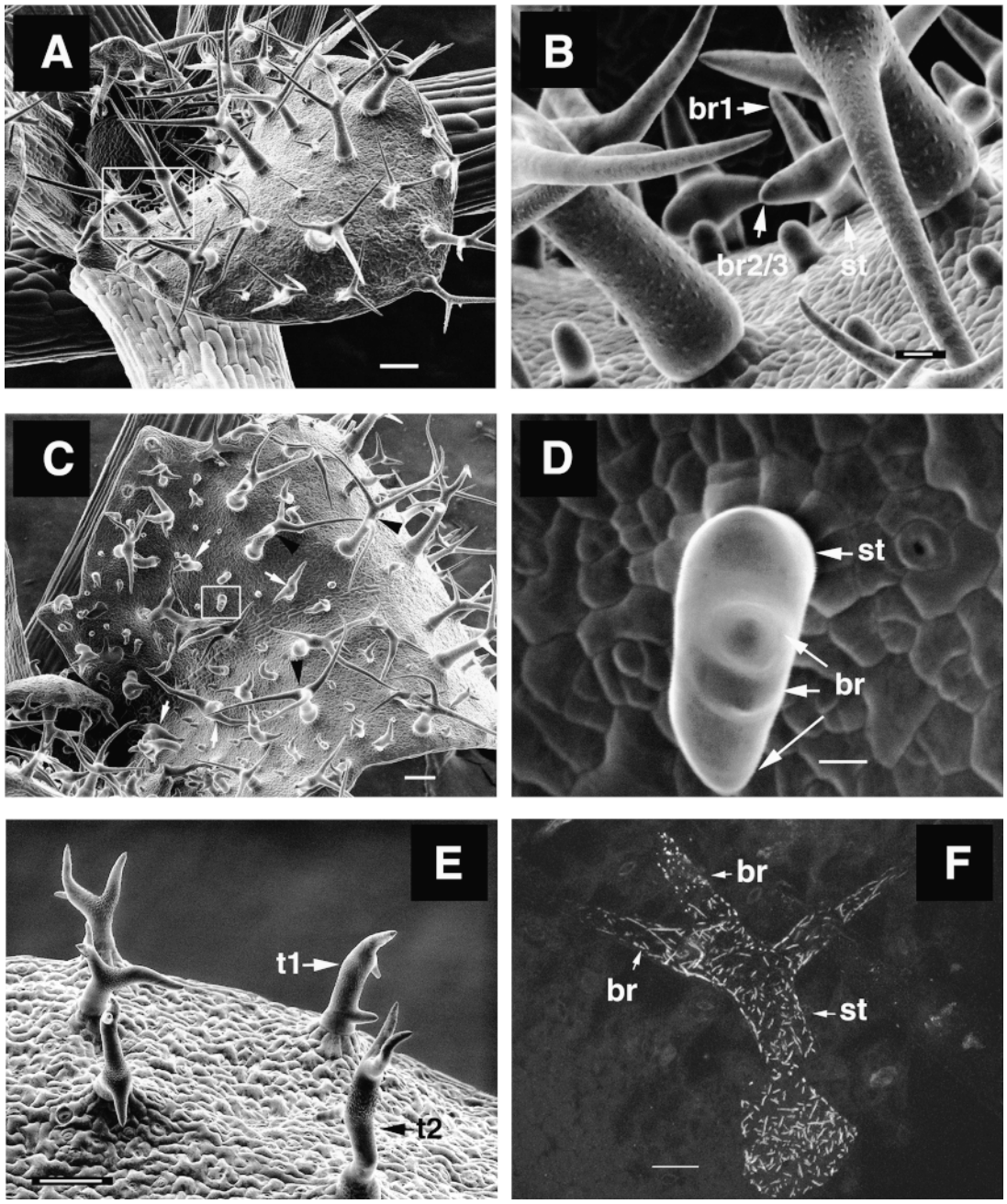

Figure 3. Effects of Cytochalasin D on Trichome Morphogenesis in Developing Leaves.

(A) Control leaves treated with buffer containing 0.1% DMSO.
(B) High magnification of developing trichomes in the boxed region in **(A)**.
(C) Leaf 48 hr after treatment with cytochalasin D. Black arrowheads indicate unaffected stage 6 trichomes. White arrows indicate trichomes with defective morphology.
(D) High magnification of the boxed region in **(C)**.
(E) Leaf 5 days after cytochalasin D treatment.
(F) Trichome actin filament organization in a cytochalasin D–treated cell.
br, branch; st, stalk; t, trichome. Bars in **(A)**, **(C)**, **(E)**, and **(F)** = 50 μm; bars in **(B)** and **(D)** = 10 μm.

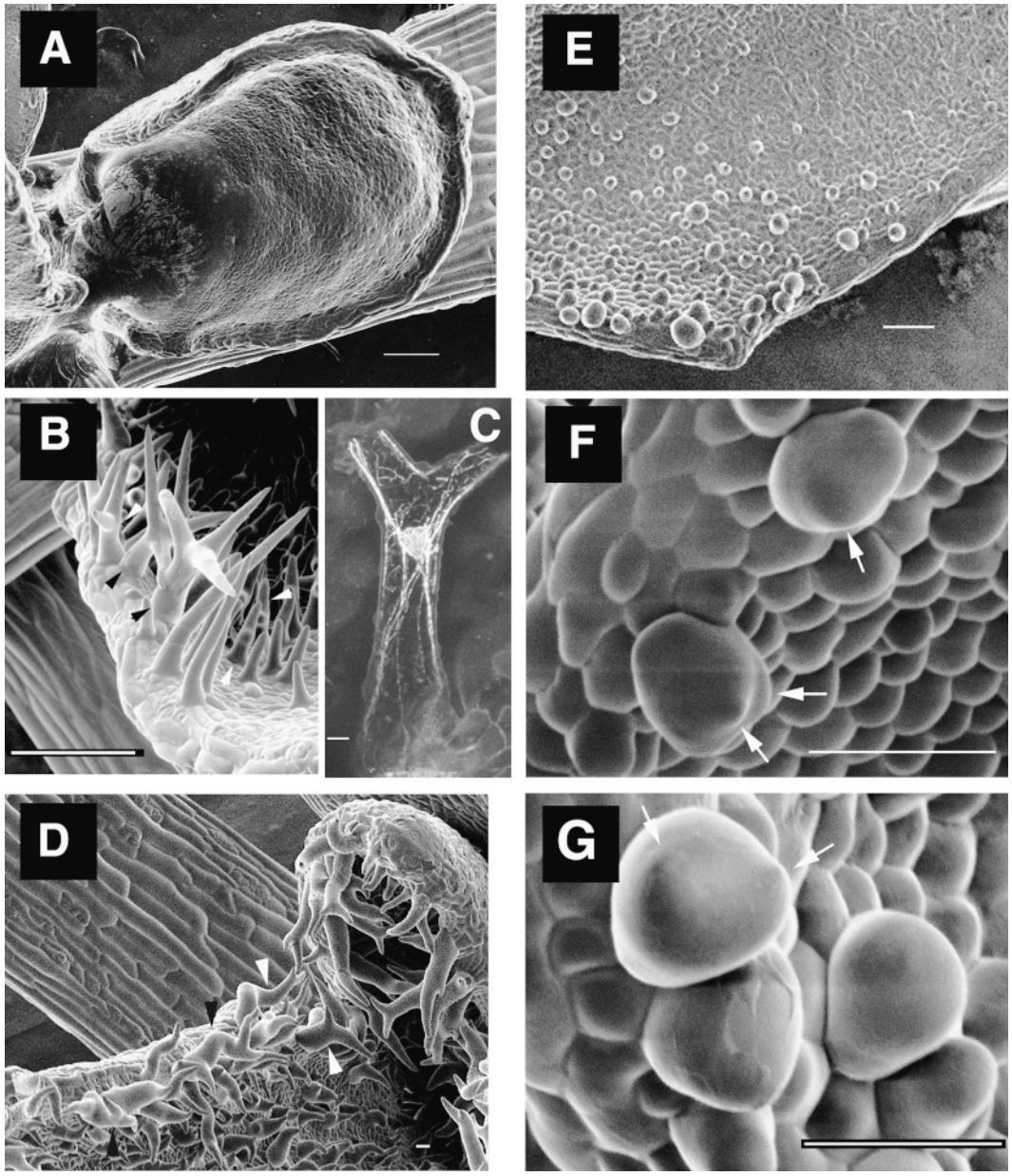

Figure 4. Effects of Cytoskeleton Inhibitors on Polar Outgrowth, Branch Initiation, and Morphogenesis in Developing Trichomes.

Effects of cytochalasin D and oryzalin on early morphogenetic events were examined in a transgenic line in which trichome initiation is dexamethasone inducible. All plants in this experiment have the genotype *ttg* 35S::*R-GR.*

(A) Developing leaf of an uninduced plant 48 hr after treatment with buffer containing 0.1% DMSO.

(B) Developing leaf 48 hr after dexamethasone induction.

(C) Actin immunolocalization in a dexamethasone-induced trichome.

(D) Developing leaf 48 hr after dexamethasone induction in the presence of cytochalasin D.

(E) Developing leaf 48 hr after dexamethasone induction in the presence of oryzalin.

(F) High magnification image of aborted trichomes induced in the presence of oryzalin.

(G) High magnification image of aborted trichomes induced in the presence of both cytochalasin D and oryzalin.

White arrowheads indicate two-branch trichomes. Black arrowheads indicate three-branch trichomes. White arrows indicate abortive trichome branch buds. Bars in **(A)**, **(B)**, and **(D)** to **(G)** = 50 μm; bar in **(C)** = 10 μm.

were swollen and distorted when initiation was induced in the presence of cytochalasin D (Figure 4D). The use of higher concentrations of cytochalasin D also did not inhibit the initiation of stalks or branches (data not shown).

The effects of cytochalasin D on trichome morphogenesis were distinct from the effects of oryzalin. Oryzalin is a plant-specific microtubule-destabilizing agent (Hugdahl and Morejohn, 1993). Pretreatment or simultaneous treatment with oryzalin did not inhibit trichome initiation after induction (Figure 4E). Trichomes that developed in the presence of oryzalin showed decreased polar growth after stage 1 (Figure 4F). The drug-treated trichomes contained bumps that might represent aborted branch buds. Cell expansion in the presence of oryzalin apparently did not require a precise F-actin organization; simultaneous exposure to cytochalasin D and oryzalin resulted in similarly shaped cells (Figure 4G).

Cytochalasin D Treatment Phenocopies the Distorted Group of Trichome Mutants

The stalk and branch morphology of cytochalasin D–treated trichomes is very similar to that of a class of trichome morphology mutants that have been referred to as the distorted group (Feenstra, 1978; Hülskamp et al., 1994). Each of the eight known distorted mutants has similar defects in trichome shape. Careful examination of the *grl* trichome phenotype by scanning electron microscopy showed the major developmental stages highlighted in Figure 5. During stages 1 and 2, trichome shape appeared normal (Figure 5A). The position of branch buds and stalk dimensions also appeared normal in stage 3 trichomes (Figures 5A and 5B). However, the phase of cell expansion after stage 3 was disrupted in *grl.* Stalk and branch diameter was often abnormally wide in stage 4 *grl* trichomes, and the apical region of the cell near the point of branch formation often showed excessive expansion (Figures 5B and 5C). Defects in stalk and branch expansion and branch position were more obvious in stage 5 cells (Figure 5C). In many cases, aberrant cell expansion occurred at or near the branch base, and some branches were aborted and remained only as nubs on the growing cell. The final shape of the cell was extremely variable; in some cases, stalk elongation appeared somewhat normal, and branch expansion was limited (Figure 5D).

Possible stage-specific differences in trichome shape in the *grl* background were examined in more detail. Measurements from a population of *grl* trichome stalks and branches were made at each developmental stage, and the plots were compared with those of the wild type. Because of the extreme variation in branch position in *grl* trichomes, stages 5 and 6 could not be identified from a discrete minimum stalk length. Therefore, stalk measurements from stages 1 to 4 (Figure 6A) and stages 5 and 6 (Figure 6B) were plotted separately. Most of the *grl* trichomes at stages 1 to 4 had cell dimensions within the range of values observed in the wild type (shown as the space enclosed by the dashed line). However, some trichomes up to stage 4 had cell widths that have not been observed in the wild type; measurements for approximately one-third of the mature *grl* trichomes fell outside the range for similarly staged wild-type trichomes (Figure 6B), and all but one of the abnormally shaped cells were overexpanded laterally relative to their length. The trend for imbalanced elongation and lateral expansion was also observed in *grl* branch structures (Figure 6E). Approximately half of the branches fell outside the range of values observed for the wild type. Two populations were apparent within the group of abnormally shaped branches: cells with abortive branches that failed to develop beyond a bud, and the commonly observed class that was disproportionately expanded in width.

To confirm the developmental stage at which cell shape defects first appear, we compared the stalk dimensions of *grl* trichomes at stages 1 to 4 with those of wild-type cells. In stages 1 and 2, 96% of the *grl* trichomes fell within the wild-type range of measurements (Figure 6C), the exceptions being two cells in stage 1, which is the most difficult stage in which to measure cell length. *grl* trichomes at stages 3 and 4 frequently had swollen stalks compared with the wild type (Figure 6D). Almost half of the measured cells had widths exceeding the size range of similarly staged wild-type cells, and all of the swollen-stalk cells were either late stage 3 or stage 4 cells. Three elongated stage 4 trichomes were also

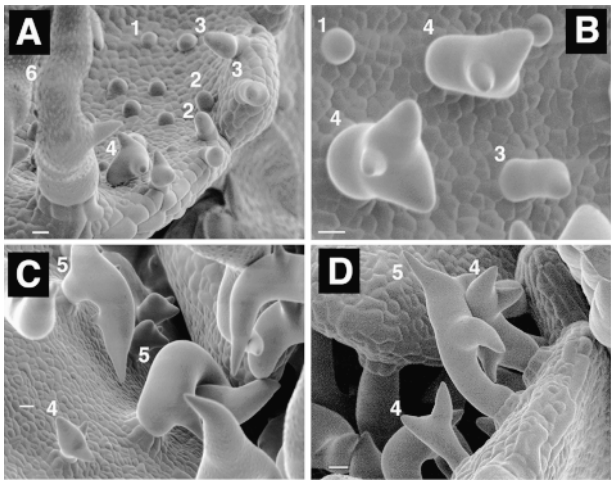

Figure 5. Phenotype of *grl* Trichomes at Different Developmental Stages.

The adaxial epidermis of leaves that contain developing mutant trichomes was examined by using scanning electron microscopy.
(A) *grl* trichomes at stages 1, 2, 3, 4, and 6.
(B) *grl* trichomes at stages 1, 3, and 4.
(C) and **(D)** *grl* trichomes at stages 4 and 5.
The numerical stage of each trichome of interest is labeled in the upper left region of the cell. Bars in **(A)** to **(D)** = 10 μm.

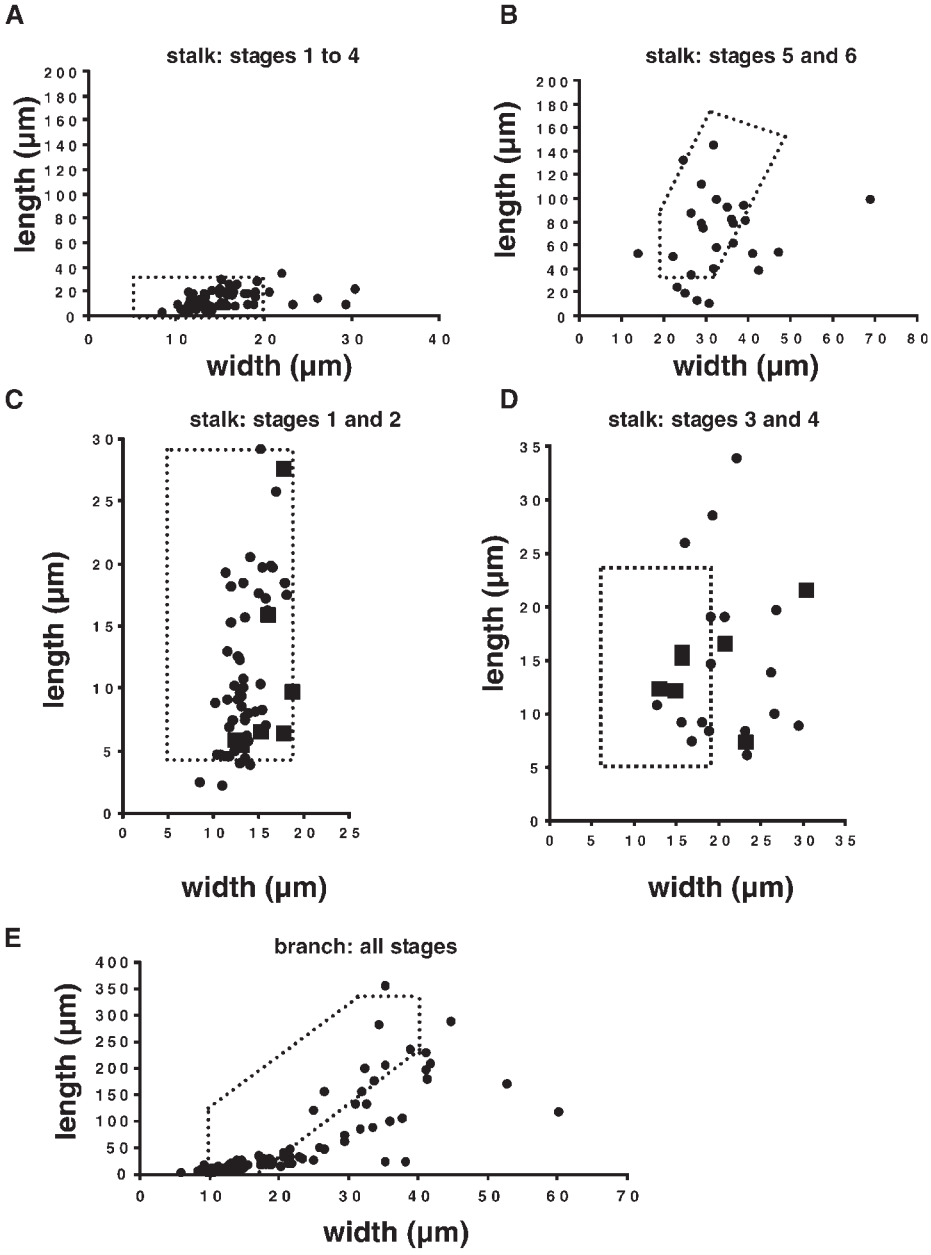

Figure 6. Dimensions of *grl* and Cytochalasin D–Treated Trichomes.

Length and width measurements of the *grl* and cytochalasin D–treated trichomes taken at all major developmental stages. Measurements were taken from static images of a population of mutant and drug-treated trichomes. Each plot graphs the length of the trichome branch or stalk (y axis) and the width (x axis). The region of the plot that contained wild-type cell dimensions at equivalent stages is partitioned with a dashed line.
(A) *grl* trichome stalk dimensions at stages 1 to 4.
(B) *grl* trichome stalk dimensions at stages 5 and 6.
(C) *grl* and cytochalasin D–treated wild-type trichome stalk dimensions at stages 1 and 2.
(D) *grl* and cytochalasin D–treated wild-type trichome stalk dimensions at stages 3 and 4.
(E) *grl* trichome branch dimensions at all stages.
In **(C)** and **(D)**, filled circles are dimensions of *grl* trichomes and filled squares are dimensions of cytochalasin D–treated wild-type trichomes.

identified (Figure 6D). Defects or delays in the transition from stage 4 to stage 5 branch tip morphology could explain this class of elongated cells (e.g., see Figure 5D). Thus, the effect of the *grl* mutation on trichome morphogenesis was first detected during the transition from stage 3 to stage 4.

We next wanted to determine whether cytochalasin D treatment had similar stage-specific effects on trichome development in wild-type plants. Trichome measurements from scanning electron microscopic images of stage 1 and stage 2 drug-treated cells are plotted in Figure 6C. None of the stage 1 and stage 2 cytochalasin D–treated cells fell outside the range of wild-type values, although width measurements appeared to be skewed toward higher values. Three of seven cytochalasin D–treated trichomes at stages 3 and 4 had diameters that were not observed in the wild-type population (Figure 6D). Each of the cells with shape defects were in either late stage 3 or stage 4.

The *grl* Mutant Has an Altered Actin Cytoskeleton

These results are consistent with the idea that actin organization is important to coordinate the pattern of cell expansion at or near the transition from stage 3 to stage 4. A defect in the organization or polymerization dynamics of F-actin could contribute to the *grl* trichome phenotype and lead to a steady state difference in the cytoskeleton of *grl* trichomes. As an initial test of this hypothesis, the actin cytoskeleton was examined in *grl* trichomes before (stage 2), during (stage 3/4), and after (stage 6) the onset of cell shape defects. In stage 2 *grl* trichomes, F-actin consisted of very loosely organized filaments or bundles that were less apparent near the tip of the cell (Figure 7A). Spherical bodies, some of which contained brightly fluorescent actin signal, were observed along the length of the cell. A top view of a late stage 3/4 *grl* trichome that had initiated three branches is shown in Figure 7B. The stalk diameter of this *grl* trichome was ~20 μm, slightly more than the highest values measured for wild-type cells at that stage. At or near the onset of the swollen phenotype, clear differences from wild-type actin organization were apparent. The largest branch displayed polarized elongation, and its aligned actin filaments terminated proximal to the branch tip and were faintly visible throughout the cytoplasm of branch 1. However, the next branches to develop, branches 2 and 3, were contained within a homogeneous region of stronger punctate and diffuse actin signals that spanned the entire apical face of the trichome. This pattern differed from the precise spatial segregation of F-actin organization observed in wild-type trichomes at stages 3 and 4.

After stage 4, *grl* trichomes expand in a fairly unpredictable manner, with stalk and branches varying in size and position from cell to cell. As one might expect, actin localization in regions of *grl* trichomes with severe morphological defects detected many randomly oriented actin bundles. Figure 7C shows a cell overexpanded at the stalk–branch junction. Actin bundles in this region of the cell did not display the organization seen in the wild type (Figures 2F and 2H), and the putative cortical attachments here were extensive. Interestingly, the stalk of the trichome shown in Figure 7C is highly polarized and similar in shape to that of the wild type. The net alignment of actin bundles reflected this polarity, but the regular spacing and strict parallel alignment of bundles observed in stage 6 wild-type trichomes was not seen here, even in the subset of *grl* trichomes that had normal stalk shape. This point is reinforced in Figures 7E and 7F. The stalk of this *grl* trichome was highly polarized, and its shape was indistinguishable from that of the wild type. The overall alignment of the actin cytoskeleton was parallel; however, numerous transverse and highly branched actin bundles were present (Figure 7E). Several three- and four-way actin bundle junctions are shown at higher magnification in Figure 7F. These structures were often observed in wild-type trichomes but only infrequently in the elongated stalks of stage 6 cells. The trichome shown in Figure 7C also contained an aborted branch with an extensive actin cytoskeleton, which is shown at higher magnification in Figure 7D.

DISCUSSION

In Arabidopsis, developmental cues are integrated with a complex morphogenetic program to construct a leaf trichome. A spherical trichome precursor cell ~6 μm in diameter develops into a multibranched cell that can grow to as long as 500 μm (Figure 1). During trichome development, initiation cues, cell expansion, endoreduplication (DNA synthesis without cytokinesis), and intercellular and intracellular transport are somehow coordinated during the regular changes in cell shape. The requirement for at least 24 genes for normal trichome growth reflects the complexity of the process. Because trichome development includes so many important aspects of plant cell growth, it is being used in several laboratories as a genetic system in which to begin to understand the control mechanisms of cell expansion and regulated growth. This study demonstrates the importance of F-actin during the maintenance and coordination of polarized cell growth and establishes Arabidopsis trichome development as a powerful model process in which to study the functions of the genes that regulate cell shape in plants.

Actin Immunolocalization and Trichome Growth

A survey of the actin organization in trichomes at each developmental stage revealed two basic relationships between actin and morphological transitions in trichomes. (1) In regions of the cell in which pattern is being established, such as branch buds and the apical regions of stage 2 stalks, the actin signal is diffuse. In branch buds and the stage 2 stalk

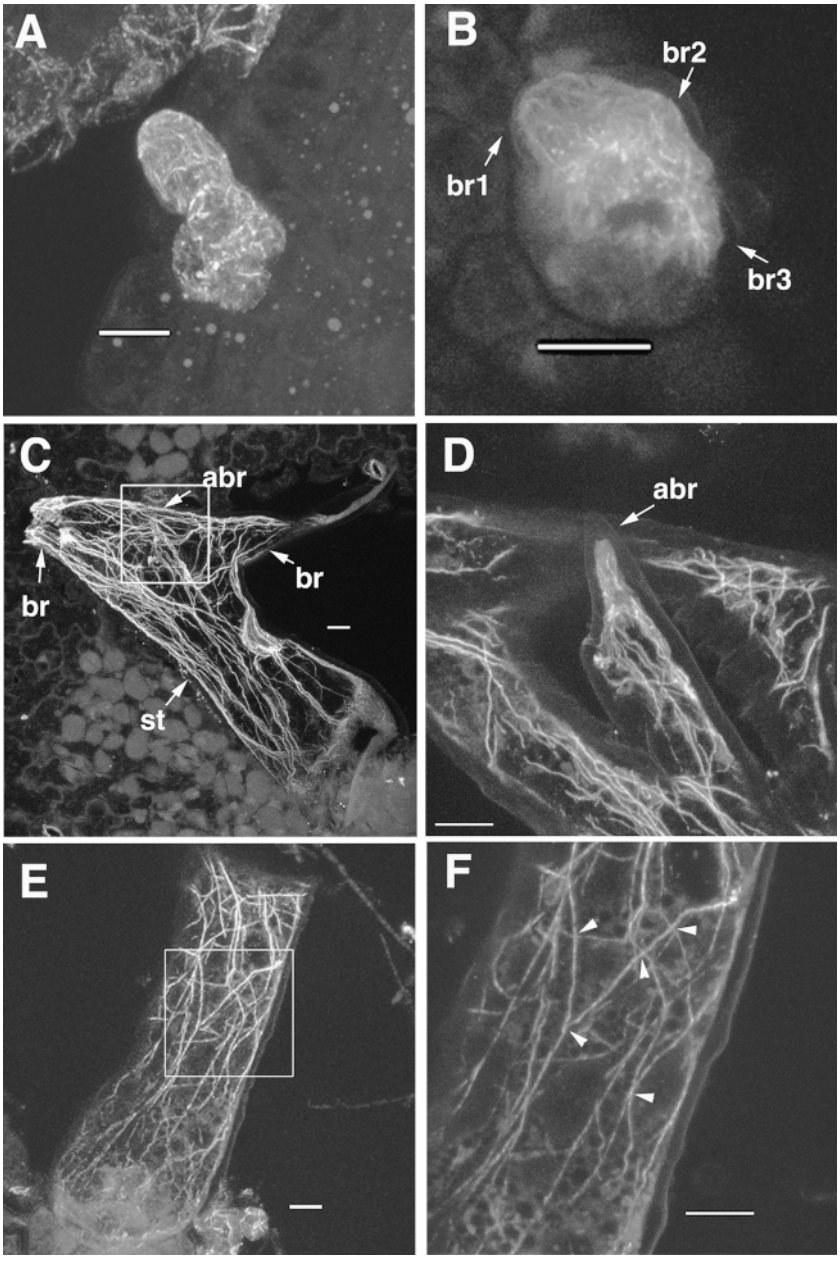

Figure 7. Actin Filament Organization in Developing and Mature *grl* Trichomes.

(A) to **(F)** each contain a maximum projection of a stack of confocal images.
(A) Side view of a late stage 2 trichome.
(B) Top view of a stage 3 trichome. Branches are numbered on the basis of differences in size.
(C) Side view of a stage 6 mutant trichome including the stalk and the base of two major branches and an abortive branch. The boxed area contains an aborted branch structure that is shown at higher magnification in **(D)**.
(D) High magnification of the actin structure in an aborted branch.
(E) Side view of an elongated stalk with wild-type dimensions. The boxed region is shown at higher magnification in **(F)**.
(F) High magnification of the intersecting actin bundles. Arrowheads indicate points of actin bundle intersection.
abr, aborted branch; br, branch; st, stalk. Bars in **(A)** to **(F)** = 10 μm.

tip, the onset of cell pattern is apparent, given the clear morphological landmarks in cell wall shape. The absence of obvious structured F-actin in these regions of the cell is similar to what is observed in the tips of growing pollen tubes (Miller et al., 1996). (2) Subsequently, in other cellular domains in which the growth pattern is established, such as the branches at stages 4 or 5 or the stage 6 stalk, F-actin dominates the anti-actin signal and is generally aligned with the growth axis. This is consistent with a subsequent role for F-actin during the reinforcement and maintenance of cell pattern in trichome development.

The arrangement and location of filamentous and nonfilamentous actin are under strict spatial control within a given cell. This is most evident during the transition from stage 3 to stage 4 (Figure 2D). In stage 3 branch buds, the actin signal is very strong and diffuse. Either the local population of F-actin is too dynamic to capture with current fixation methods, or a localized high concentration of unpolymerized actin dominates the signal obtained with the anti-actin antibodies. The diffuse signal may reflect the localization of globular (G)-actin–sequestering proteins or a pool of unpolymerized actin. The image of F-actin in Figure 2D clearly shows that just 20 μm away from the branch bud, an expanding stage 4 branch displays a polarized F-actin system with a reduced diffuse actin signal at the tip. Similar compartmentalization of F-actin has been observed in tip-growing pollen tubes (Miller et al., 1996; Kost et al., 1998).

In contrast to growing pollen tubes, stage 3 trichomes contain three separate elongation domains that appear to undergo similar rearrangements of F-actin: each domain sequentially executes a highly regulated branch initiation and maintenance program. How the spatial control of actin polymerization and organization is achieved during branch growth is not known, but almost certainly actin binding proteins are involved. For example, the maize actin-depolymerizing factor (ADF) ZmADF3 is localized to a restricted apical elongation domain in root hairs (Jiang et al., 1997). Arabidopsis ADF1 increases actin polymerization dynamics in vitro (Carlier et al., 1997). Perhaps tight spatial control of proteins such as ADF has a functional role during trichome morphogenesis.

At each stage of trichome development, the actin cytoskeleton contains actin filaments or fine bundles. After stage 1, most of these bundles are aligned with the local axis of elongation. Similar aligned arrays of fine actin bundles have been observed in a variety of elongating cell types (reviewed in Heslop-Harrison et al., 1986; Thimann et al., 1992; Jackson and Heath, 1993). Even after cell expansion has ceased, stage 6 trichomes display fine, parallel arrays of evenly spaced F-actin bundles.

Several groups have proposed that the presence of fine actin bundles, as opposed to heavy bundles of aggregated filaments, is associated with the ability to transport vesicles (Franke et al., 1972; Thimann et al., 1992; Foissner et al., 1996; Waller and Nick, 1997; Wang and Nick, 1998; Miller et al., 1999). The detection of actin-associated spherical bodies at all developmental stages and the observation of rapid longitudinal vesicle transport along the cortex of living stage 6 trichomes (D.B. Szymanski, unpublished results) are consistent with this idea.

The mode of cell expansion during trichome morphogenesis has not been directly addressed, and more than one growth mechanism is likely to be involved. For example, stage 2 trichomes may elongate by way of a tip growth mechanism. During stage 2, the cells increase in length without significant radial expansion (Figure 1B), and a dense population of spherical bodies ~1 μm in diameter can be detected near the cell tip (Figure 2C). Stage 2 trichomes resemble the growth aspect and cellular organization of tip-growing cells, such as pollen tubes and fungal hyphae (Jackson and Heath, 1993; Miller et al., 1996). The population of spherical bodies appears to be heterogeneous; a subset of them displayed a strong actin signal. Perhaps some of the fluorescence signal was artifactual, reflecting imperfect fixation. However, the actin-positive spherical bodies we detected were in regions of the cell that appeared to be well preserved. Furthermore, these spheres did not have the "beads on string" pattern seen when F-actin is artificially destabilized (Thimann et al., 1992). Perhaps delivery of polymerization-competent actin toward the trichome tip reinforces the control of localized cell expansion at later stages of development. Moreover, a role for intercalary cell expansion cannot be ruled out during stage 2. Pulse labeling or microscopic wall-marking experiments must be conducted to define the precise domains of cell expansion in developing trichomes.

Tip growth mechanisms alone do not generate the shape of a mature trichome. During stage 5, stalk length and diameter increase in a highly regular manner along the entire cell surface. By definition, this is diffuse growth, not tip growth. Furthermore, it is difficult to imagine how localized regions of expansion after stage 4 could give rise to a stage 6 cell. During stage 5, an extremely fine uniform network of actin filaments was detected throughout the trichome (Figure 2E); perhaps this network is important for regulated transport of materials to the cell perimeter.

The images of F-actin provide a general description of the major changes in actin organization during trichome development. However, many questions about how the intricate actin cytoskeleton in mature trichomes is constructed remain unanswered. For example, in stage 6 trichomes, the actin signal was found almost exclusively in aligned F-actin bundles, some of which exceeded 100 μm in length and ran from the cell stalk into the branches (Figures 2F and 2H). Stalks and branches at earlier stages of development displayed a dense population of very fine F-actin filaments or bundles. Which proteins regulate the reorganization of actin bundles in the transition from stage 5 to stage 6? Do the filaments from earlier stages coalesce to form larger bundles in the mature cell, or is there additional assembly during later stages? Are the filaments in each bundle coaligned or are they antiparallel? Unlike Drosophila bristles, static images

of actin structure in developing trichomes do not yield a clear model of actin bundle assembly. In the Drosophila bristle, discrete bundles of actin ~3 μm long stack end to end during bristle growth (Tilney et al., 1996), and gaps in the bristle bundles occur during both the assembly and the disassembly process. No such bundle modules were detected in trichome stalks or branches. An analysis of F-actin ultrastructure and changes in F-actin in living trichomes may help resolve some of these questions.

Stage-Specific Cytoskeletal Requirements

At each stage of trichome development, the pattern of F-actin organization correlates with the patterns of cell elongation, but the functional significance of the actin arrays up to late stage 3 or stage 4 is not clear. Stage 1 trichomes expand isodiametrically, and both cytoplasmic reticulate F-actin and cortical arrays were detected at this stage (Figures 1A and 1B). During polarized expansion perpendicular to the plane of the leaf, developing stage 2 trichomes contain a population of loosely aligned actin filaments that terminate proximal to the cell tip. However, neither stage 1 nor stage 2 trichomes display obvious sensitivity to cytochalasin D. The result cannot be explained by a cytochalasin D–dependent arrest of cell elongation. First, cytochalasin D treatment does not noticeably affect the rate or pattern of cell elongation in dexamethasone-induced trichomes up to late stage 3 or 4. Second, trichomes at stages 1 and 2 do not accumulate in cytochalasin D–treated wild-type plants. The effects of cytochalasin D on trichomes are visible within 30 min, and the drug markedly alters the F-actin organization in all epidermal cell types. However, even after 24 hr of cytochalasin D treatment, polymerized actin is not always completely eliminated. Perhaps F-actin is either relatively unimportant through stage 3, or its function does not strictly depend on a specific organization. Subtle effects of cytochalasin D on stage 2 growth will have to be examined by using live cell imaging.

Morphogenesis during stages 1 and 2 is dramatically affected by the microtubule-destabilizing agent oryzalin: in the presence of oryzalin, both induced (Figure 4F) and normally developing trichomes (data not shown) fail to initiate an organized polar outgrowth or well-defined branch buds. The expansion that occurs in the presence of oryzalin is generally unaffected by the condition of the actin cytoskeleton (Figure 4G) and most likely represents isotropic expansion of the apical portion of the trichome that is not impeded by surrounding socket cells. Microtubule-dependent polarizing activity appears to act upstream of actin-dependent activity during trichome development. These specific effects of the cytoskeleton-disrupting drugs on trichome growth are distinct from their effects on pollen tube growth and embryo pattern formation in brown algae; the latter processes are extremely sensitive to actin-destabilizing drugs but relatively tolerant to microtubule-destabilizing agents. Understanding the interplay between microtubule and F-actin function during trichome development is a key future challenge. Unfortunately, reliable examination of microtubule organization in trichomes has not been possible, and efforts to develop methods to colocalize microtubules and microfilaments are ongoing.

In a polarized cell, the maintenance and propagation of a growth pattern are fundamental components of cell shape control (Drubin and Nelson, 1996), and the effect of cytochalasin D on trichome development is consistent with a role for F-actin in these processes. Similar conclusions have been drawn with respect to the role of actin during bristle development in Drosophila (Tilney et al., 1995). In both wild-type and induced trichomes, the coordinated expansion of the stalks and branches after stage 4 is sensitive to cytochalasin D; growth is not completely inhibited, but stalks become swollen, and in many cases, branch elongation is aborted (Figures 3C, 6D, and 6E). At the cellular level, these effects mirror the tissue-level inhibition of elongation that has been observed after treatment with cytochalasins (Thimann et al., 1992; Baskin and Bivens, 1995; Wang and Nick, 1998). At stage 4, branch initiation is completed, and the basic body plan of the cell has been defined; the final phase includes the coordinated elongation and expansion of defined stalk and branch structures. Possibly, precisely organized actin filaments or bundles are essential for the proper delivery of construction materials during this phase of trichome development.

grl Trichome Morphogenesis

The class of mutants termed the distorted group possess trichomes with striking similarity to cytochalasin D–treated cells. In both drug-treated and *grl* trichomes, abnormal stalk swelling and expansion along the apical face of the cell often occur during the transition to stage 4. These similar shape defects exist despite the fact that the F-actin organization in *grl* does not at all resemble that of cytochalasin D–treated cells (Figure 7). F-actin–dependent activities appear to be highly constrained during the transition to the elongation and expansion phase (stages 4 and 5), and subtle defects in actin organization or cellular function can have dramatic effects on subsequent cell shape.

At or near the onset of the distorted trichome phenotype at stage 4, the actin signal in *grl* differs from that of the wild type. A strong diffuse and punctate actin signal is distributed throughout the apical portion of the cell (Figure 7B). At this point, we do not know whether these differences in actin organization are the direct cause of the mutant phenotype, but the mislocalization of structures that contribute to cell expansion could explain the cell shape defects in the mutant.

Stage 6 *grl* trichomes contain extensive F-actin arrays. Intricate networks of F-actin have been identified in abortive branches, in overexpanded branches, and in regions of the

cell that appear somewhat normal. A simple absence of actin polymerization cannot explain any aspect of the mutant phenotype. However, the severity of cell shape defects is reflected in the increasingly random organization of F-actin bundles (Figure 7). Even in the most normally shaped domains of stage 6 *grl* trichomes, actin bundles tend to be more branched than they are in the wild type and lack the regular spacing around the perimeter of the cell. Perhaps the *grl* mutation causes subtle defects in F-actin organization, the consequences of which may vary stochastically from cell to cell or within any given cell.

The relationship among cell growth, *GRL* gene function, and actin organization remains to be determined. For example, defects in the *GRL* gene could either directly or indirectly affect actin organization. Furthermore, the *grl* allele used in this study could be a mild loss-of-function mutation in an essential gene that regulates cellular organization in many cell types. Analysis of the *GRL* gene product and its relationship to actin organization will help to address these questions.

Conclusion

The F-actin–dependent phase of branch and stalk expansion is complex and probably requires several components. For example, reinforcement of an established cell growth pattern may require the local delivery of a specific class of vesicles. Any mutation that alters the timing, position, or rate of delivery could cause a breakdown in coordinated cell growth; the list of candidate genes is long. The existence of at least eight trichome mutants with a similar distorted phenotype is consistent with the idea that several components are required to coordinate F-actin–dependent branch and stalk elongation after stage 4. Further analysis of this group of genes will undoubtedly lead to a more mechanistic understanding of plant cell growth control.

METHODS

Scanning Electron Microscopy and Cell Measurements

The shoots from intact plants were frozen in liquid nitrogen and observed on a microscope (model 800; Philips Electron Optics, Eindhoven, The Netherlands) equipped with a cold stage (Ahlstrand, 1996). For cell dimension measurements, the images were imported into National Institutes of Health (NIH) Image ppc v1.61 (NIH, Bethesda, MD; ftp site: ftp://codon.nih.gov/pub/nih-image/) and calibrated according to the magnification. Distances were measured in micrometers by using the line tool option. For all stalk and branch measurements, cells that appeared to be perpendicular to the plane of view were chosen for measurement. Because socket cells obscure the base of trichomes, the midpoint of the stalk was chosen as the position at which to measure width. Trichome branches elongate, but they display a decreasing diameter toward the tip; therefore, branch diameter at the base is the most reliable indicator of increased branch size at all stages of development.

Plant Strains and Growth Conditions

For all phenotypic characterizations, *Arabidopsis thaliana* seeds were surface sterilized, germinated on plates, and propagated on minimal media containing Murashige and Skoog salts (Life Technologies, Gaithersburg, MD), 1% sucrose, and 0.8% Bacto agar (Life Technologies). Growth chambers were maintained at 22°C with constant illumination at 80 μE m^{-2} sec^{-1}. The wild-type strain used was ecotype Columbia. The *grl* distorted mutant was a gift from M. Hülskamp (Universität Tübingen, Germany). *grl* was isolated in the Landsberg *erecta* background (Hülskamp et al., 1994) and was outcrossed to Columbia plants for these experiments. The *ttg* 35S::*R-GR* plants were a gift from A. Lloyd (University of Texas, Austin).

Cytoskeletal Inhibitor Treatment and Dexamethasone Induction

Cytochalasin D (Sigma) was diluted from a 10 mM stock in DMSO. A 2-μL drop of 50 μm cytochalasin D in 0.1% DMSO was placed on the adaxial surface of developing leaves. Oryzalin (Lilly Research Laboratories, Greenfield, IN) was prepared from a 20 mM stock in DMSO. Oryzalin was effective between 10 and 100 μM and was used at 100 μM in the 48-hr induction experiments. Plants were maintained at 100% humidity throughout the treatment. The fifth and sixth leaves of wild-type plants and leaves three and four of *ttg* 35S::*R-GR* plants were treated with cytochalasin D. In the induction experiments, a 10-μM solution of dexamethasone in 0.1% DMSO was applied either alone or with inhibitors.

Immunolabeling and Fluorescence Microscopy

Shoot-derived tissue was harvested and submerged in either 100% methanol or 2.5% formaldehyde (prepared from paraformaldehyde), 0.5% glutaraldehyde, 0.1 μM *m*-maleimido benzoyl *N*-hydroxy succinimide ester in PEMT (100 mM Pipes-KOH, pH 6.9, 5 mM EGTA, 2 mM $MgCl_2$, and 0.05% Triton X-100) for 1 hr at room temperature. Tissue was rinsed twice in PEMT, mounted between two glass slides, and frozen in liquid nitrogen. Frozen shoots were crushed between two aluminum blocks maintained at −80°C (Wasteneys et al., 1997). Crushed samples were filtered through coarse metal mesh and washed three times for 10 min in PBS, pH 7.0, containing 0.01% Triton X-100 and 25 mM glycine (PBSTG). Leaves were then suspended in permeabilization buffer containing PBS and 1% Triton X-100 for 1 to 2 hr. The monoclonal IgM anti-actin antibody N350 (Boehringer Mannheim, Indianapolis, IN) (1:400) or monoclonal IgG anti-actin antibody C4 (ICN Pharmaceuticals, Costa Mesa, CA) (1:100) was used to label actin. After two 10-min washes in PBSTG, fluorescein isothiocyanate–conjugated secondary antibodies were used at a 1:200 dilution. After three washes in PBS, samples were mounted in Vectashield (Vector Laboratories, Burlingame, CA) and viewed on a confocal microscope (model MRC 1024; Bio-Rad Research Laboratories, Hercules, CA) based on a Nikon Diaphot (Nikon Corp., Tokyo, Japan) inverted microscope. Signal was obtained by using the 488-nm laser line, and fluorescent light was filtered through a 510 ± 15-nm bandpass filter. Images were manipulated by using NIH Image. Final figures were composed by using Adobe Photoshop version 5.0 (Adobe Systems Inc., Mountain View, CA).

ACKNOWLEDGMENTS

The St. Paul Campus Microscopy and Imaging Consortium provided excellent facilities and technical support. Thanks to Daniel Budge and Beth Kent for editorial assistance. D.B.S. was supported by National Science Foundation (NSF) Cytoskeleton Training Grant No. DBI 96002237. This work was also supported by a Cooperative Research, Education, and Extension Service USDA Grant to D.B.S. and NSF/Integrative Biology and Neuroscience Grant No. 9506192 to M.D.M.

Received July 14, 1999; accepted October 4, 1999.

REFERENCES

Ahlstrand, G. (1996). Low-temperature low-voltage scanning microscopy (LTLVSEM) of uncoated frozen biological materials: A simple alternative. In Proceedings of Microscopy Microanalysis, G.W. Bailey, J. Corbett, R. Dimlich, J. Michael, and N. Zaluzec, eds (San Francisco, CA: San Francisco Press), pp. 918–919.

Alessa, L., and Kropf, D.L. (1999). F-actin marks the rhizoid pole in living *Pelvetia compressa* zygotes. Development **126,** 201–209.

An, Y.Q., Huang, S., McDowell, J.M., McKinney, E.C., and Meagher, R.B. (1996a). Conserved expression of the Arabidopsis *ACT1* and *ACT3* actin subclass in organ primordia and mature pollen. Plant Cell **8,** 15–30.

An, Y.Q., McDowell, J.M., Huang, S., McKinney, E.C., Chambliss, S., and Meagher, R.B. (1996b). Strong, constitutive expression of the *Arabidopsis ACT2*/*ACT8* actin subclass in vegetative tissues. Plant J. **10,** 107–121.

Baker, B., Zambryski, P., Staskawicz, B., and Dinesh-Kumar, S.P. (1997). Signaling in plant–microbe interactions. Science **276,** 726–733.

Baskin, T.I., and Bivens, N.J. (1995). Stimulation of radial expansion in Arabidopsis roots by inhibitors of actomyosin and vesicle secretion but not by various inhibitors of metabolism. Planta **197,** 514–521.

Bender, H. (1960). Studies on the expression of various *singed* alleles in *Drosophila melanogaster.* Genetics **45,** 867–883.

Brawley, S.H., and Robinson, K.R. (1985). Cytochalasin treatment disrupts the endogenous currents associated with cell polarization in fucoid zygotes: Studies of the role of F-actin in embryogenesis. J. Cell Biol. **100,** 1173–1184.

Cant, K., Knowles, B.A., Mooseker, M.S., and Cooley, L. (1994). *Drosophila* singed, a fascin homolog, is required for actin bundle formation during oogenesis and bristle extension. J. Cell Biol. **125,** 369–380.

Carlier, M.F., Laurent, V., Santolini, J., Melki, R., Didry, D., Xia, G.X., Hong, Y., Chua, N.-H., and Pantaloni, D. (1997). Actin depolymerizing factor (ADF/cofilin) enhances the rate of filament turnover: Implication in actin-based motility. J. Cell Biol. **136,** 1307–1322.

Cho, S.-O., and Wick, S.M. (1990). Distribution and function of actin in the developing stomatal complex of winter rye (*Secale cereale* cv. Puma). Protoplasma **157,** 154–164.

Cho, S.-O., and Wick, S.M. (1991). Actin in the developing stomatal complex of winter rye: A comparison of actin antibodies and rh-phalloidin labeling of control and CB-treated tissues. Cell Motil. Cytoskel. **19,** 25–36.

Cooper, J.A. (1987). Effects of cytochalasin and phalloidin on actin. J. Cell Biol. **105,** 1473–1478.

Dolan, L., Janmaat, K., Willemsen, V., Linstead, P., Poethig, S., Roberts, K., and Scheres, B. (1993). Cellular organisation of the *Arabidopsis thaliana* root. Development **119,** 71–84.

Drubin, D.G., and Nelson, W.J. (1996). Origins of cell polarity. Cell **84,** 335–344.

Fankhauser, C., and Chory, J. (1997). Light control of plant development. Annu. Rev. Cell Dev. Biol. **13,** 203–229.

Feenstra, W.J. (1978). Contiguity of linkage groups I and IV as revealed by linkage relationship of two newly isolated markers *dis-1* and *dis-2.* Arab. Inf. Serv. **15,** 35–38.

Foissner, I., Lichtscheidl, I.K., and Wasteneys, G.O. (1996). Actin-based vesicle dynamics and exocytosis during wound wall formation in characean internodal cells. Cell Motil. Cytoskel. **35,** 35–48.

Folkers, U., Berger, J., and Hülskamp, M. (1997). Cell morphogenesis of trichomes in *Arabidopsis*: Differential control of primary and secondary branching by branch initiation regulators and cell growth. Development **124,** 3779–3786.

Franke, W.W., Herth, W., Van Der Woude, W.J., and Morre, D.J. (1972). Tubular and filamentous structures in pollen tubes: Possible involvement as guide elements in protoplasmic streaming and vectorial migration of secretory vesicles. Planta **105,** 317–341.

Gilliland, L.U., McKinney, E.C., Asmussen, M.A., and Meagher, R.B. (1998). Detection of deleterious genotypes in multigenerational studies. I. Disruptions in individual *Arabidopsis* actin genes. Genetics **149,** 717–725.

Hable, W.E., and Kropf, D.L. (1998). Roles of secretion and the cytoskeleton in cell adhesion and polarity establishment in *Pelvetia compressa* zygotes. Dev. Biol. **198,** 45–56.

Heslop-Harrison, J., Heslop-Harrison, Y., Cresti, M., Tiezzi, A., and Ciampolini, F. (1986). Actin during pollen tube germination. J. Cell Sci. **86,** 1–8.

Hopmann, R., Cooper, J.A., and Miller, K.G. (1996). Actin organization, bristle morphology, and viability are affected by actin capping protein mutations in *Drosophila.* J. Cell Biol. **133,** 1293–1305.

Hugdahl, J.D., and Morejohn, L.C. (1993). Rapid and reversible high-affinity binding of the dinitroanaline herbicide oryzalin to tubulin from *Zea mays* L. Plant Physiol. **102,** 725–740.

Hülskamp, M., Misra, S., and Jürgens, G. (1994). Genetic dissection of trichome cell development in Arabidopsis. Cell **76,** 555–566.

Jackson, S.L., and Heath, I.B. (1993). The dynamic behavior of cytoplasmic F-actin in growing hyphae. Protoplasma **173,** 23–34.

Jiang, C.J., Weeds, A.G., and Hussey, P.J. (1997). The maize actin-depolymerizing factor, ZmADF3, redistributes to the growing tip of elongating root hairs and can be induced to translocate into the nucleus with actin. Plant J. **12,** 1035–1043.

Kost, B., Spielhofer, P., and Chua, N.-H. (1998). A GFP–mouse talin fusion protein labels plant actin filaments *in vivo* and visualizes the actin cytoskeleton in growing pollen tubes. Plant J. **16,** 393–401.

Lancelle, S.A., Cresti, M., and Hepler, P.K. (1987). Ultrastructure of the cytoskeleton in freeze-substituted pollen tubes of *Nicotiana alata.* Protoplasma **140,** 141–150.

Larkin, J.C., Oppenheimer, D.G., and Marks, M.D. (1994). The *GL1* gene and the trichome developmental pathway in *Arabidopsis thaliana.* In Results and Problems in Cell Differentiation: Plant Promoters and Transcription Factors, L. Nover, ed (Berlin: Spinger-Verlag), pp. 259–275.

Larkin, J.C., Young, N., Prigge, M., and Marks, M.D. (1996). The control of trichome spacing and number in *Arabidopsis.* Development **122,** 997–1005.

Larkin, J.C., Marks, M.D., Nadeau, J., and Sack, F. (1997). Epidermal cell fate and patterning in leaves. Plant Cell **9,** 1109–1120.

Lloyd, A.M., Schena, M., Walbot, V., and Davis, R.W. (1994). Epidermal cell fate determination in *Arabidopsis*: Patterns defined by a steroid-inducible regulator. Science **266,** 436–439.

Marks, M.D. (1997). Molecular genetic analysis of trichome development in Arabidopsis. Annu. Rev. Plant Physiol. Plant Mol. Biol. **48,** 137–163.

Mascarenhas, J.P., and LaFountain, J. (1972). Protoplasmic streaming, cytochalasin B, and growth of the pollen tube. Tissue Cell **4,** 11–14.

Masucci, J.D., Rerie, W.G., Foreman, D.R., Zhang, M., Galway, M.E., Marks, M.D., and Schiefelbein, J.W. (1996). The homeobox gene *GLABRA2* is required for position-dependent cell differentiation in the root epidermis of *Arabidopsis thaliana.* Development **122,** 1253–1260.

McCurdy, D.W., and Williamson, R.E. (1991). Actin and actin-associated proteins. In The Cytoskeletal Basis of Plant Growth and Form, C.W. Lloyd, ed (San Diego, CA: Academic Press), pp. 3–14.

McDowell, J.M., An, Y.Q., Huang, S., McKinney, E.C., and Meagher, R.B. (1996). The Arabidopsis *ACT7* actin gene is expressed in rapidly developing tissues and responds to several external stimuli. Plant Physiol. **111,** 699–711.

Miller, D.D., Lancelle, S.A., and Hepler, P.K. (1996). Actin microfilaments do not form a dense meshwork in *Lilium longiflorum* pollen tubes. Protoplasma **195,** 123–132.

Miller, D.D., de Ruijter, N.C.A., Bisseling, T., and Emons, A.M.C. (1999). The role of actin in root hair morphogenesis: Studies with lipochito-oligosaccharide as a growth stimulator and cytochalasin as an actin perturbing drug. Plant J. **17,** 141–154.

Narasimhulu, S.B., and Reddy, A.S.N. (1998). Characterization of microtubule binding domains in the Arabidopsis kinesin-like calmodulin binding protein. Plant Cell **10,** 957–965.

Oppenheimer, D.G., Pollock, M.A., Vacik, J., Szymanski, D.B., Ericson, B., Feldmann, K., and Marks, M.D. (1997). Essential role of a kinesin-like protein in *Arabidopsis* trichome morphogenesis. Proc. Natl. Acad. Sci. USA **94,** 6261–6266.

Palevitz, B.A. (1993). Morphological plasticity of the mitotic apparatus in plants and its developmental consequences. Plant Cell **5,** 1001–1009.

Picton, J.M., and Steer, M.W. (1981). Determination of secretory vesicle production rates by dictysomes in pollen tubes of *Tradescantia* using cytochalasin D. J. Cell Sci. **49,** 261–272.

Pyke, K.A., Marrison, J.L., and Leech, R.M. (1991). Temporal and spatial development of the cells of the expanding first leaf of *Arabidopsis thaliana* (L.) Heynh. J. Exp. Bot. **42,** 1407–1416.

Quatrano, R.S. (1973). Separation of processes associated with differentiation of two-celled *Fucus* embryos. Dev. Biol. **30,** 209–213.

Song, H., Golovkin, M., Reddy, A.S., and Endow, S.A. (1997). In vitro motility of AtKCBP, a calmodulin-binding kinesin protein of *Arabidopsis.* Proc. Natl. Acad. Sci. USA **94,** 322–327.

Staiger, C.J., Gibbon, B.C., Kovar, D.R., and Zonia, L.E. (1997). Profilin and actin-depolymerizing factor: Modulators of actin organization in plants. Trends Plant Sci. **2,** 275–281.

Szymanski, D.B., and Marks, M.D. (1998). *GLABROUS1* overexpression and *TRIPTYCHON* alter the cell cycle and trichome cell fate in Arabidopsis. Plant Cell **10,** 2047–2062.

Szymanski, D.B., Jilk, R.A., Pollock, S.M., and Marks, M.D. (1998). Control of *GL2* expression in *Arabidopsis* leaves and trichomes. Development **125,** 1161–1171.

Thimann, K.V., Reese, K., and Nachmias, V.T. (1992). Actin and the elongation of plant cells. Protoplasma **171,** 153–166.

Tilney, L.G., Tilney, M.S., and Guild, G.M. (1995). F-actin bundles in *Drosophila* bristles. I. Two filament cross-links are involved in bundling. J. Cell Biol. **130,** 629–638.

Tilney, L.G., Connelly, P., Smith, S., and Guild, G.M. (1996). F-actin bundles in *Drosophila* bristles are assembled from modules composed of short filaments. J. Cell Biol. **135,** 1291–1308.

Verheyen, E.M., and Cooley, L. (1994). Profilin mutations disrupt multiple actin-dependent processes during *Drosophila* development. Development **120,** 717–728.

Waller, F., and Nick, P. (1997). Response of actin microfilaments during phytochrome-controlled growth of maize seedlings. Protoplasma **200,** 154–162.

Wang, Q.-Y., and Nick, P. (1998). The auxin response of actin is altered in the rice mutant Yin-Yang. Protoplasma **204,** 22–33.

Wasteneys, G.O., Willingale-Theune, J., and Menzel, D. (1997). Freeze shattering: A simple and effective method for permeabilizing higher plant cell walls. J. Microsc. **188,** 51–61.

Woeste, K., and Kieber, J.J. (1998). The molecular basis of ethylene signaling in *Arabidopsis.* Philos. Trans. R. Soc. Lond. **353,** 1431–1438.